ELSEVIER

Catalysis Today 54 (1999) 229–243

CATALYSIS TODAY

www.elsevier.com/locate/cattod

Photocatalytic treatment of phenol and 2,4-dichlorophenol in a solar plant in the way to scaling-up

J. Giménez *, D. Curcó, M.A. Queral

Departamento de Ingeniería Química, Facultad de Química, Universidad de Barcelona, C/Martí i Franquès, 1. 08028-Barcelona, Spain

Abstract

The photocatalytic treatment of phenol and 2,4-dichlorophenol (2,4-DCP) has been tested by using titania in suspension as catalyst. Experiments were done at the solar facilities of the Plataforma Solar de Almería (Spain). Two experimental devices were used: CPCs modules; and flat reactor. Reaction kinetics is order one with respect to the pollutant (phenol or 2,4-DCP) concentration. Two different kinetic constants were fitted from experimental data by considering only time influence on the reaction rate or by considering the radiation influence and assuming that reaction rate is proportional to the square root of photonic flow. In all cases, kinetic constant increases when catalyst concentration does it, reaches a maximum (at 0.5 g/l of catalyst in the CPCs case, and at 0.2 g/l in the flat case), and after this maximum, decreases. When kinetic constants obtained in the two utilities tested are compared, important differences were found when only dependence on time is considered. However, results improve when radiation influence is considered, and the values obtained in both devices are more close. This fact indicates the influence of reactor geometry and radiation on the reaction rate, and their importance in the scaling-up. Finally, the efficiencies of CPCs and flat reactor are compared attending to the collector area needed to obtain the same conversion in the pollutant treatment. It seems that CPCs work better, however several factors can influence (for instance, weather: cloudy or sunny days) and more accurate studies are needed. ©1999 Elsevier Science B.V. All rights reserved.

Keywords: Photocatalysis; Photocatalytic oxidation; Pullutants treatment; Radiation models; Reactor modelling

1. Introduction

Photocatalysis can be an useful technique in the treatment of several pollutants. Studies have been carried out at laboratory level, and also at pilot plant scale, showing the efficiency of photocatalytic methods in the removal of organic and inorganic contaminants [1–6]. However, comparison between results obtained by different researchers is difficult, because experimental parameters are different. That is, when reactor geometry, radiation sources and operating conditions are not the same. Thus, parameters have to be estimated so that comparison can be made. In addition, the problem arises not only from the comparisons, may be the most important problem is that one referred to the extrapolation of results from one experimental device to another, and the use of these results in the scaling-up.

The question is how to choose parameters that allow to compare and scaling-up. The most important fact differentiating photocatalytic processes from classical heterogeneous catalysis processes is the presence of light. This means that the role played by light has to be quantified, and the parameters defining it have to be introduced into the model describing the system. The reason is that, in photocatalytic processes, the catalyst

* Corresponding author. Tel.: +34-93-402-1293; fax: +34-93-402-1291.
E-mail address: gimenez@angel.qui.ub.es (J. Giménez)

0920-5861/99/$ – see front matter ©1999 Elsevier Science B.V. All rights reserved.
PII: S0920-5861(99)00185-6

(semiconductor) needs to absorb radiation to generate the electron/hole (e^-/h^+) pairs able to catalyze the corresponding redox reactions.

On this way, let us to consider the solution of the problem in successive steps beginning from the classical kinetic equations. In any photocatalytic process, the reaction rate can be expressed in different forms considering different parameters. If only time influence on the concentration evolution is considered, the reaction rate is defined by equations like:

$$r = kf(c) \quad (1)$$

where r is the reaction rate ($\mathrm{mol\,l^{-1}\,s^{-1}}$), k the global kinetic constant, and $f(c)$ a function of concentration, normally, a Langmuir–Hinshelwood–Hougen–Watson function [7–18].

Expressions like Eq. (1) are valid only for the experimental device used and fixed experimental conditions, such as constant radiation reaching the reactor. That is, k varies when reactor geometry or radiation source or operating conditions are changed. This means that k is not useful for comparison between devices and for scaling-up.

A first improvement, with respect to Eq. (1), consists in the consideration of the radiation arriving (F_i) at the surface of the collectors (walls of photoreactor, mirrors, reflectors, etc.) of photoreactor:

$$r = k_i f(c) f_i(F_i) \quad (2)$$

where $f_i(F_i)$ is a function of radiation arriving at the system, and k_i a new kinetic constant different from k.

For sure, k_i has more wide applications than k, but important parameters such as reactor geometry have not been yet considered. Thus, more steps are needed. The next one is to consider the radiation entering (F_e) the photoreactor:

$$r = k_e f(c) f_e(F_e) \quad (3)$$

where $f_e(F_e)$ is a function of radiation entering the photoreactor, and k_e a new kinetic constant different from k and k_i.

This new kinetic constant, k_e, improves the model and allows us to consider the influence of the reactor geometry on the radiation entering the reaction chamber.

Considering all that mentioned above, in this paper we have studied, as reactions model, the photocatalytic oxidation of phenol and 2,4-dicholorophenol (2,4-DCP). Experiments were carried out at pilot plant scale in the facilities of the PSA (Plataforma Solar de Almería, Spain), by using solar radiation. Data obtained are used to evaluate the radiation entering the systems and to estimate the kinetic constant k_e, useful in the way to scaling-up. Two different experimental devices have been used that allows us to prove the goodness of the kinetic constants estimated, and also the experimental and computational ways proposed to evaluate the entering radiation.

2. Experimental

All the experiments have been done in the facilities installed at the PSA and these facilities have been already described in other papers and technical reports [19–25]. However, a simple and schematic view of experimental devices is shown in Figs. 1 and 2.

Several CPCs modules were used, being connected in series and mounted on a fixed platform, at a 37° angle (from ground) and facing south, to maximize its performance (the PSA is at +37° latitude). Each CPC module is 1.22 m wide and 1 m long and consists of eight parallel CPC reflectors (152 mm wide) with UV-transparent tubular receivers (ID 48 mm). The total volume of the system is 247 l, and the volume useful for reaction is 108 l.

As shown in Fig. 1, in the CPCs, a solution of phenol or 2,4-DCP with TiO_2 (Degussa P-25) in suspension was prepared in the reservoir tanks and fed to the photoreactors. The system operated in a discontinuous mode and recirculating the solution. High flow rates (minimum $3.5\,\mathrm{m^3\,h^{-1}}$) were used and perfect mixing flow can be assumed. By using these experimental conditions, the photodegradation achieved for the phenol or 2,4-DCP was higher than in other conditions (for instance, plug flow), and data treatment becomes easier. The oxygen necessary for the phenol or 2,4-DCP oxidation enters the reaction medium by stirring in reservoir tanks.

The flat reactor is a cylindrical tank (see Fig. 2) of 1.26 m diameter and 8 cm height, that means a volume of 100 l. Several tubes are located at the bottom of it, through which circulates an air-flow, bubbling in the solution to be treated through the holes made in the tubes. In the flat reactor, the system operates in a discontinuous mode. Thus, the solution of phenol or

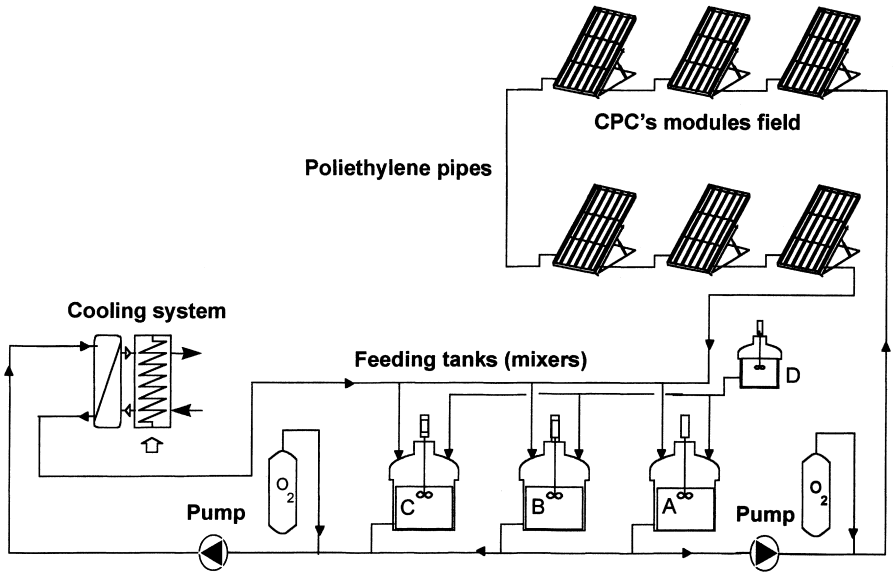

Fig. 1. Schematic view of PSA detoxification loop with CPCs modules.

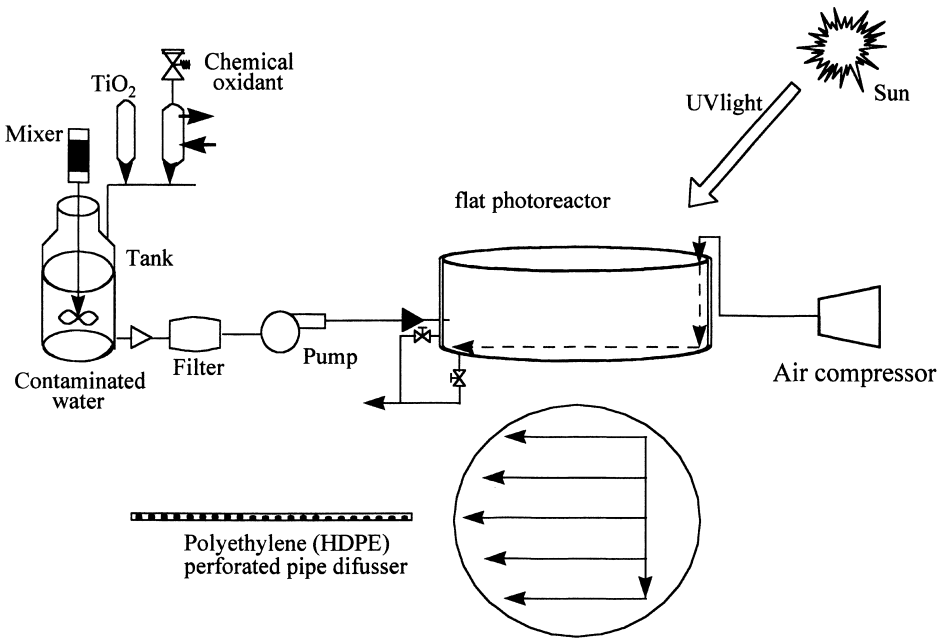

Fig. 2. Schematic view of PSA detoxification loop with flat reactor.

2,4-DCP with TiO_2 in suspension was prepared into the reactor, and the catalyst was maintained in suspension by using the air stream, as it was mentioned before. The air flow is high enough to assure a good stirring and perfect mixing flow can be considered. Also, air supplies the oxygen necessary for the phenol or 2,4-DCP oxidation. Other possibility to maintain catalyst in suspension, supplying the oxygen necessary, is to recirculate continuously the suspension by using a centrifugal pump, external to the tank. Both

Table 1
Experiments of photocatalytic degradation of phenol in CPCs modules and flat reactor

Experiment[a]	c_p[b] (g/l)	pH_0[c]	pH_f[d]	c_0[e] (ppm)	c_f[f] (ppm)	t[g] (h)	X[h]
PF03	0.1	4.4	4.2	31	18	6	0.41
PF04	0.1	4.0	3.9	33	21	6	0.38
PF05	0.1	4.2	4.0	38	23	6	0.38
PF08	0.2	4.0	3.9	25	12	5.75	0.51
PF09	0.2	4.2	4.3	12	6	6	0.54
PF10	0.2	4.2	4.1	33	18	6	0.46
PF11	0.5	3.3	3.2	23	13	5	0.42
PF12	1	3.8	4.0	33	25	5	0.24
PC02	0.1	3.3	3.8	29	11	6	0.62
PC03	0.2	4.1	3.7	33	6	6	0.80
PC04	0.5	3.2	3.2	29	4	6	0.87
PC05	1	4.5	3.7	29	8	5	0.71

[a] Experiment number.
[b] Catalyst concentration.
[c] Initial pH.
[d] Final pH.
[e] Initial concentration of phenol.
[f] Final concentration of phenol.
[g] Total time for the experiment.
[h] Percentual conversion.

Table 2
Experiments of photocatalytic degradation of 2,4-DCP in the CPCs modules and flat reactor

Experiment[a]	c_p[b] (g/l)	pH_0[c]	pH_f[d]	c_0[e] (ppm)	c_f[f] (ppm)	t[g] (h)	X[h]
DF01	0.1	6.6	7/4	56	46	4	0.18
DF02	0.1	6.2	5.5	96	80	6	0.17
DF03	0.2	5.9	3.9	93	67	5	0.28
DF04	0.5	6.2	4.3	9.1	62	4	0.32
DF05	0.5	7.6	4.9	98	79	5.5	0.19
DF06	1	5.9	4.8	96	66	4.5	0.31
DF07	2	5.6	4.3	94	60	4.5	0.36
DC01	0.1	4.6	3.6	89	46	4	0.48
DC02	0.1	5.9	3.4	89	44	6	0.51
DC03	0.2	4.2	3.2	86	33	4	0.62
DC04	0.5	4.2	3.4	91	29	4	0.68
Dc05	0.5	5.9	4.2	94	61	5.5	0.35
DC06	1	6.0	3.9	91	41	4.5	0.55
DC07	2	5.1	3.9	90	41	4.5	0.54

[a] Experiment number.
[b] Catalyst concentration.
[c] Initial pH.
[d] Final pH.
[e] Initial concentration of phenol.
[f] Final concentration of phenol.
[g] Total time for the experiment.
[h] Percentual conversion.

systems can ensure perfect mixing flow and good oxygenation.

For each pollutant testing and in each experimental device, catalyst (TiO_2) concentration was varied between 0 and 2 g/l.

These two devices provide us experimental data under different experimental conditions, because the use of different geometry (tubular and flat) implies a different radiation model in each system. In addition and referring to the radiation field, low concentrating systems (CPCs modules) can be compared with systems without light concentration (flat reactor).

Phenol and 2,4-DCP were analyzed by HPLC, following the methodology already described in previous papers [22]. TOC measurements were also carried out for each sample. The pH measurements were also made because they provide additional data, because in the 2,4-DCP case, for example, its degradation produces HCl, and pH has to decrease according to 2,4-DCP degradation.

3. Results and discussion

The results obtained in the photocatalytic degradation of phenol and 2,4-DCP are summarized in Tables 1 and 2, respectively, for both experimental devices used (CPCs and flat reactor). In each experiment, several samples were taken during time, and the evolution of concentration was followed.

The conversion (X), appearing in Tables 1 and 2, is calculated from the experimental data, according to the expression:

$$X = \frac{c_0 - c(t)}{c_0} \tag{4}$$

where c_0 is the initial concentration of pollutant, and $c(t)$ the pollutant concentration at time t.

As an example, Figs. 3 and 4 show the evolution of the phenol and 2,4-DCP concentration during time for experiments carried with a catalyst concentration of 0.5 g/l. The behaviour observed is the same for the other catalyst concentrations tested.

According to literature and previous research of this group, it is known that kinetics for phenol and 2,4-DCP photooxidation follows a first order dependence with respect to the phenol or 2,4-DCP concentration in the experimental conditions tested [7–9,11,15,17,18,22,24,26,27]. The equation to be used for the fitting of Tables 1 and 2 data depends on

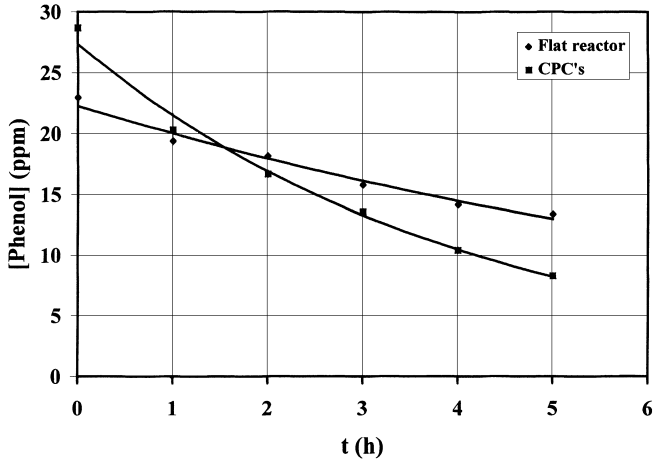

Fig. 3. Evolution of phenol concentration during time for experiments carried out in the flat reactor and in the CPCs modules at a catalyst concentration of 0.5 g/l (experiments PF07 and PC03 in Table 1).

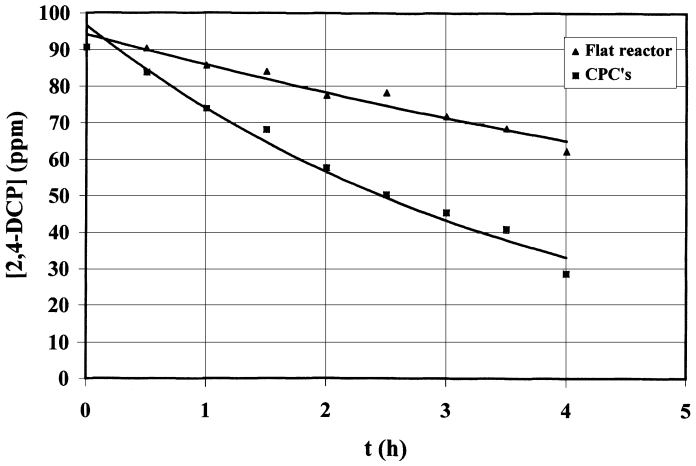

Fig. 4. Evolution of 2,4-DCP concentration during time for experiments carried out in the flat reactor and in the CPCs modules at a catalyst concentration of 0.5 g/l (experiments DF04 and DC04 in Table 2).

the flow model for the photoreactor. As commented in Section 2, perfect mixing flow model can be assumed here, for both reactors tested (CPCs and flat). Thus, mass balance for phenol or 2,4-DCP, assuming first order kinetics, drives to the equation:

$$\frac{dc}{dt} = -kc \tag{5}$$

where k is the global kinetic constant, and c the phenol or 2,4-DCP concentration at any time. The integration of the Eq. (5) gives:

$$\ln(c) = \ln(c_0) - kt \tag{6}$$

Thus, if logarithm of the concentrations represented in Figs. 3 and 4 are depicted in front of time, a linear relationship will be obtained. Fig. 5 shows the results obtained when titania concentration was 0.5 g/l. Similar results were obtained for the other catalyst concentrations.

The global kinetic constant can be obtained from the slope of the straight lines fitted for each experiment, that is, for each catalyst concentration. Variation of these global kinetic constants on catalyst concen-

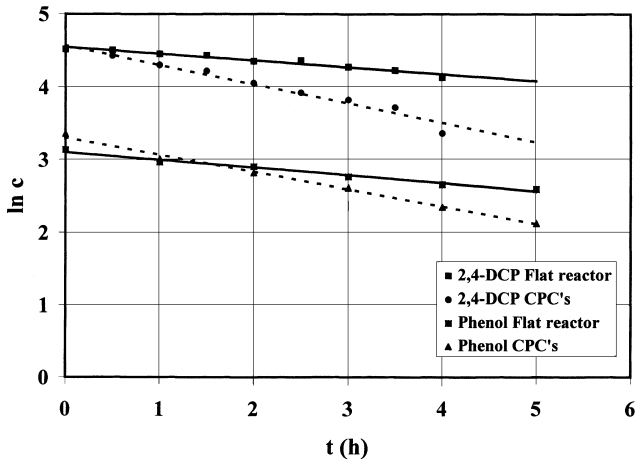

Fig. 5. Linearization of the variation of concentration of phenol or 2,4-DCP on time for experiments done in the flat reactor and in the CPCs modules at a catalyst concentration of 0.5 g/l (experiments shown in Figs. 3 and 4).

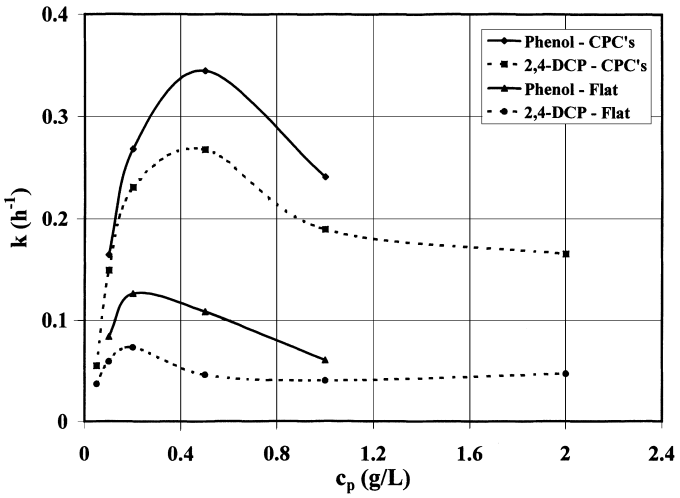

Fig. 6. Variation of the global kinetic constant (k) on catalyst concentration for experiments carried out in the flat reactor and in the CPCs modules with phenol and 2,4-DCP (experiments of Tables 1 and 2).

tration is indicated in Fig. 6. It can be observed that the kinetic constant increases as catalyst concentration does, reaching a maximum. This maximum appears at values of c_p around 0.5 g/l in the case of CPCs, for both pollutants tested, and at values of c_p around 0.2 g/l in the case of flat reactor. This fact points out the need of to consider the reactor geometry. For concentrations higher than this value, kinetic constant values begin to decrease. This behaviour has been observed in other photocatalytic processes, for instance in the hydrogen photoproduction from water photolysis and sulfides [28–31]. Some reasons can explain this fact. For catalyst concentrations higher than a certain value (for example 0.2 or 0.5 g/l here) not all the catalyst particles can see the light. Particles nearest to the surface of reactor can shade particles in the deep and/or can produce light scattering. On this way, both phenomena could drive to a decrease in the reaction rate.

From Fig. 6, it seems that CPCs give higher reaction rates than flat reactor. However, just to now, only the

influence of time on the reaction rate has been considered. That is, only the dependence of reaction rate (r) on phenol concentration has been taken into account, according to the function:

$$r = kc \tag{7}$$

As it was indicated in Section 1, when the reaction rate is expressed by Eq. (1) or Eq. (7), the influence of the radiation entering the system is not considered. This influence can be taken into account by using expressions like Eq. (3) ($r = k_e f(c) f_e(F_e)$). This topic will be developed in the next sections, and the specific expressions for Eq. (3) will be deduced establishing different kinds of dependence between the reaction rate and the radiation entering the system.

3.1. Calculation of reactors efficiency

The first step will be the study of the radiation field for the different reactors tested. That implies to use the actinometric and radiometric data for radiation calculations. The second step will be to introduce the radiation data into the Eq. (3) and calculate the k_e kinetic constants.

As already explained in previous papers [22,24], the radiation arriving at the surface of radiation collector (F_i, eins/s) can be expressed as:

$$F_i = \frac{S_{col}}{N_a h c_v} W_T(t) \sum_{\lambda_{min}}^{\lambda_{max}} \lambda f_\lambda \tag{8}$$

S_{col} is the CPCs or flat area able to receive radiation (m^2), N_a the Avogadro's number (6.023×10^{23}), λ the wavelength (m), h the Planck's constant (6.63×10^{-34} J s), c_v the light rate (3×10^8 m/s), λ_{min} the minimum wavelength in the spectrum of the radiation source and λ_{max} the maximum wavelength that can be absorbed by the solution into the photoreactors and/or that allows to the generation of e^-/h^+ pairs, $W_T(t)$ is the global radiation reaching the surface of the collectors of the system at time t (W/m^2), and f_λ the fraction of global radiation at the λ wavelength, which is known from the radiation data obtained at the PSA by using a LICOR 1800 spectroradiometer, as explained in previous papers [22–24,32,33].

However, only part of the radiation arriving at the experimental system enters the photoreactor. The relationship between radiation entering and radiation arriving at the surface of collectors depends on the geometrical characteristics of the experimental device.

In the case of CPCs modules, the area S_{col} can be expressed as a function of the area of each CPCs module (S_{mod}, 1.22 m^2) and the number (n_{mod}) of modules (two in our case):

$$S_{col} = S_{bmod} n_{bmod} \tag{9}$$

In addition, the relationship between F_i and F_e can be established through two factors: the efficiency factor (Φ_{ef}) and the transmittance factors ($\Phi_{T\lambda}$). The first one is related to the characteristics of the system such as reactor geometry and position with respect to the sun, which are considered independent on the wavelength (the reflectance of the CPCs mirrors depends only slightly on the wavelength). The transmittance factor depends on the material (Teflon) from which the walls of the photoreactor (CPCs modules) are made, and it depends on the wavelength. Thus, by considering Equations (8) and (9), and the last two factors defined, the radiation entering the CPCs modules (F_e, eins/s) can be expressed as:

$$F_e = \frac{\Phi_{ef} S_{bmod} n_{bmod}}{N_a h c_v} W_T(t) \sum_{\lambda_{min}}^{\lambda_{max}} \lambda f_\lambda \Phi_{T\lambda} \tag{10}$$

The transmittance factor ($\Phi_{T\lambda}$) for the walls of the photoreactor comes from data provided by the supplier its values are already listed in previous papers [22]. The efficiency factor (Φ_{ef}) has to be calculated for each experimental system (CPCs modules here). The procedure followed is based on the actinometric reaction between the oxalic acid and uranile salt, as explained in previous papers [22,23,32–34]. This actinometric reaction has been widely described in the literature, and it has been demonstrated that the reaction is zero order with respect to the oxalic acid concentration [35–37], if conversion is lower than 20%. Thus, the reaction rate is directly related to the radiation absorbed by the actinometer:

$$r = \frac{dc}{dt} = f(F_{abs}) \tag{11}$$

where r is the reaction rate (mol l^{-1} s^{-1}), c the oxalic acid concentration (mol/l) at time t (s), and F_{abs} the radiation absorbed by the actinometer (eins/s).

The radiation absorbed can be related to the radiation entering by taking into account the optical way followed by the radiation, and the absorption coefficient (α_λ, cm^{-1}) for the reaction medium at each wavelength. By considering Eq. (10), the radiation absorbed by the actinometer can be expressed as:

$$F_{abs} = \frac{\Phi_{ef} S_{bmod} n_{bmod}}{N_a h c_v} W_T(t) \times \sum_{\lambda_{min}}^{\lambda_{max}} (\lambda f_\lambda [1 - \exp(-\alpha_\lambda D)] \Phi_{T\lambda}) \quad (12)$$

where D is the optical pathway, assumed to be equal to the tube diameter (4.8 cm).

Following Eq. (11), the reaction rate can be expressed as a function of the radiation absorbed (Eq. (12)) taking into account the quantum yield (ϕ_λ) at each wavelength for this actinometer:

$$\frac{dc}{dt} = -\frac{\Phi_{ef} S_{bmod} n_{bmod}}{V_T N_a h c_v} W_T(t) \times \sum_{\lambda=300}^{546} (\lambda f_\lambda [1 - \exp(-\alpha_\lambda D)] \phi_\lambda \Phi_{T\lambda}) \quad (13)$$

where V_T is the total volume of the system (170 l, only two CPCs modules were used).

λ_{min} and λ_{max} have been replaced by 300 and 546 nm, because 300 nm is the minimum wavelength for the radiation used, and 546 nm is the upper wavelength where this actinometer can absorb radiation. The quantum yield (ϕ_λ) and the absorption coefficient (α_λ) are reported in literature for this actinometric reaction [35,37].

The integration of Eq. (13) is:

$$c(t) = c_0 - \frac{\Phi_{ef} S_{bmod} n_{bmod}}{V_T N_a h c_v} W_T \times \sum_{\lambda=300}^{546} (\lambda f_\lambda [1 - \exp(-\alpha_\lambda D)] \phi_\lambda \Phi_{T\lambda}) \quad (14)$$

The experimental procedure for the experimental actinometry is the following: the device used (feeding tank, pipes and two CPCs modules) was filled with an actinometric solution (0.05 M oxalic acid and 0.01 M uranyl salt). The solution was homogeneized in the dark (the modules were covered). After that, covers were removed and sunlight illuminated the modules, taking this time as zero and being c_0 the oxalic acid concentration at this moment. Samples were taken during time, and the concentration of oxalic acid ($c(t)$) was measured by permanganate titration. Simultaneously, the radiation arriving at the CPCs was measured by using a radiometer, being W_T the total radiation (J/m^2) that has arrived at the CPCs from the initial time ($t = 0$) up to the time t corresponding to the time when each sample was taken. All the questions related to the radiometric measurements have been already explained in previous papers [22,23].

All the parameters appearing in Eq. (14) are known, except Φ_{ef}. Thus, fitting of experimental c vs. radiation drives to a straight line from which slope Φ_{ef} can be calculated, being in this case 0.755. This value represents the fraction of the radiation really entering the photoreactor with respect to the maximum possible.

Similar explanations can be given for the flat reactor case with some little changes. In this case, the surface (S_{flat}, 1.25 m^2) over which radiation incomes (S_{col} in the CPCs) is the top area of the flat reactor.) In addition, the transmittance factors ($\Phi_{T\lambda}$) are not necessary because radiation reaches directly the surface of solution, and the efficiency factor (Φ_{ef}) can be considered equal to one. Consequently, the radiation entering can be expressed by:

$$F_e = \frac{S_{flat}}{N_a h c_v} W_T(t) \sum_{\lambda_{min}}^{\lambda_{max}} \lambda f_\lambda \quad (15)$$

The actinometric experimental way to find the efficiency factor for CPCs presents however some disadvantage. For instance, it has to be assumed a constant optical path of photons through the reactor, and it is not considered that the efficiency factor could vary with the proportions of direct and diffuse radiation reaching the system. A more sophisticated way to obtain the efficiency factor and to correlate it with the fraction of diffuse radiation and the inclination of the rays reaching the device can be provided by simulation methods, which are being now developed (see, as an example, Figs. 7 and 8). This methodology allows us to calculate the efficiency factor at each time t from measurements of direct and diffuse radiation and by taking into account the day of the year, the solar hour and the geographical situation of the device. Thus, depending on the ratio between direct and diffuse radiation (different depending on the weather), the efficiency of the

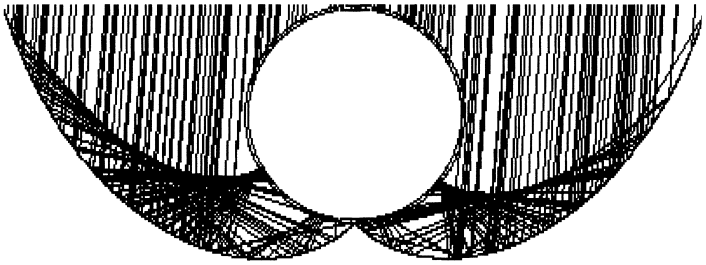

Fig. 7. Direct radiation arriving to the CPCs modules and radiation reaching the CPCs tubes with an azimuthal angle of 85°.

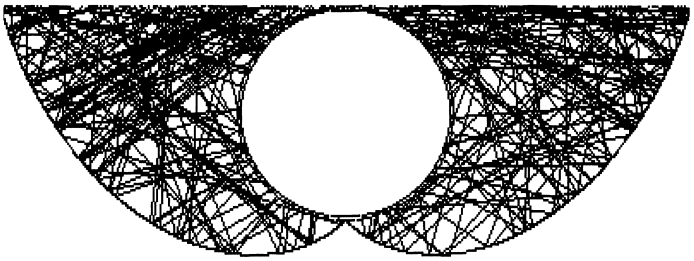

Fig. 8. Diffuse radiation arriving to the CPCs modules and radiation reaching the CPCs tubes.

CPCs can be also different (see in Figs. 7 and 8 how light arrives in different manner at the reactor).

Summarizing, Φ_{ef} can be estimated from the experimental actinometric methods or by using these simulation programs and radiation models just explained. Having determined the efficiency factor (Φ_{ef}), and with the equations described before, the CPCs modules and flat reactor are characterized from the point of view of the radiation field. Now, it is possible to estimate the amount of radiation entering the photoreactor useful for photocatalytic experiments. The semiconductor used as catalyst was TiO_2, being active in the spectral range of wavelengths between 300 and 385 nm. Then, using Eq. (10), the useful radiation entering the photoreactor in a time t can be expressed as:

$$F_e = \frac{\Phi_{ef} S_{bmod} n_{bmod}}{N_a h c_v} W_T(t) \sum_{\lambda=300}^{385} \lambda f_\lambda \Phi_{T\lambda} \qquad (16)$$

3.2. Calculation of kinetic constants

As known [9,15,16,38–40], the reaction rate depends on the photonic flow or on the square root of the photonic flow. In this case, it has been demonstrated that reaction rate depends on the square root of the photonic flow [22,24]. This means that the reaction rate can be expressed as a function of pollutant concentration and the square root of radiation absorbed in the photoreactor. That is, Eq. (3) takes now the expression:

$$\frac{dc}{dt} = k' f_a \left(F_{abs}^{1/2}\right) c \qquad (17)$$

The next question is what is the form of the function (f_a) of radiation absorbed. This can be deduced by considering the radiation absorbed (F_{abs}) in the photoreactor. If there are n_c particles of catalyst illuminated, the radiation absorbed by each particle will be F_{abs}/n_c. The radiation absorbed is proportional to radiation entering ($F_{abs} = k_1 F_e$), and the number of particles illuminated depends on the illuminated surface ($n_c = k_2 S_f$). In the CPCs, the illuminated surface can expressed by the following equation:

$$S_f = n_{bmod} n_{Tbmod} \pi D L \qquad (18)$$

where n_{Tmod} is the number of tubes in a module (8 tubes), D the diameter of a tube (4.8 cm), and L the length of a tube (100 cm).

By considering all the explained in the last paragraph, substituting Eq. (18) in Eq. (17), and taking into account that F_e is given by Eq. (10), the reaction rate can be expressed by Eq. (19). The complete details for the deduction of Eq. (19) from Eq. (17) have been already explained in previous papers [22].

$$\frac{dc}{dt} = -k_e \frac{\Phi_{ef}^{1/2} S_{bmod}^{1/2} n_{bmod} (n_{Tbmod} \pi DL)}{V_T (N_a h c_v)^{1/2}} [W_T(t)]^{1/2} c \times \left(\sum_{\lambda=300}^{385} \lambda f_\lambda \Phi_{T\lambda} \right)^{1/2} \quad (19)$$

This equation cannot be solved analytically because $W_T(t)$ changes in an unpredictable way during time when sunlight is used as radiation source. This fact can be overcame by developing Eq. (19) by the Euler's method in such way that it results:

$$c(t_{i+1}) = c(t_i) - k_e \frac{n_{bmod} (\Phi_{ef} S_{bmod} n_{Tbmod} \pi DL)}{V_T (N_a h c_v)^{1/2}} c(t_i) \times \Delta t \sum_{j=1}^{i+1} (W_T^{1/2}(t_j) \Delta t_j) \left(\sum_{\lambda=300}^{385} \lambda f_\lambda \Phi_{T\lambda} \right)^{1/2} \quad (20)$$

where Δt_j is the interval of time in which measurements of radiation are carried out (a minute in our experimental system) and Δt the interval of time between the time t_{i+1} and t_i. From here and by using linear fitting methods, k_e can be obtained. As differences of concentrations between two consecutive times t_i and t_{i+1} are small, the Euler's method is assumed to be applicable.

By fitting data of Tables 1 and 2 (Experiments PC01-PC04 and DC01-DC07) to that equation, considering W_T at each time, straight lines are obtained and, from their slopes, the kinetic constants k_e can be calculated for each experiment. The values for these kinetic constants are depicted in Fig. 9.

A similar discussion can be done for the flat reactor but, here, the illuminated surface (S_f) is S_{flat}. Then, by taking into account that radiation entering is given now by the Eq. (15), the reaction rate can be expressed as:

$$\frac{dc}{dt} = -k_e \frac{S_{flat}}{V_T (N_a h c_v)^{1/2}} [W_T(t)]^{1/2} c \left(\sum_{\lambda=300}^{385} \lambda f_\lambda \right)^{1/2} \quad (21)$$

As commented for the CPCs, the integration of this equation, by using the Euler's method, drives to:

$$c(t_{i+1}) = c(t_i) - k_e \frac{S_{flat}}{V_T (N_a h c_v)^{1/2}} c(t_i) \Delta t \times \sum_{j=i}^{i+1} \left(W_T^{1/2}(t_j) \Delta t_j \right) \left(\sum_{\lambda=300}^{385} \lambda f_\lambda \right)^{1/2} \quad (22)$$

By fitting data of Tables 1 and 2 (Experiments PF03-PF08, DF01-DF07), in the same manner than in CPCs case, to Eq. (22), straight lines are also obtained and, from their slopes, the kinetic constants k_e can be calculated for each experiment. The values for these kinetic constants are depicted in Fig. 9.

3.3. Comparison between both reactors

Comparisons between the reactors can be made by regarding different parameters: the kinetic constants or the collector area needed to achieve a given conversion. Here, the kinetic constants obtained for all the experimental devices tested are considered. The values are depicted in Figs. 6 and 9.

It may be easily observed (see Fig. 6) that it is difficult to establish a clear trend in the kinetic constants calculated by considering only time. However, results improve when reaction rate is assumed to be proportional to the square root of the radiation entering. In this case (see Fig. 9), the values obtained for the kinetic constants are closer to each other comparing the reactors used. For that, from now we will work with the kinetic constants calculated assuming that reaction rate is proportional to the square root of the radiation entering.

As commented before, the values of the kinetic constants depend on the device. Thus, kinetic constant increases as catalyst concentration does, and reaches a maximum around a value of c_p that varies depending on the device (see Figs. 4 and 5). The maximum appears at a catalyst concentration of 0.2 g/l for the flat reactor, and at 0.5 g/l for the CPCs. These differences can be attributed to the different geometry (tubular or

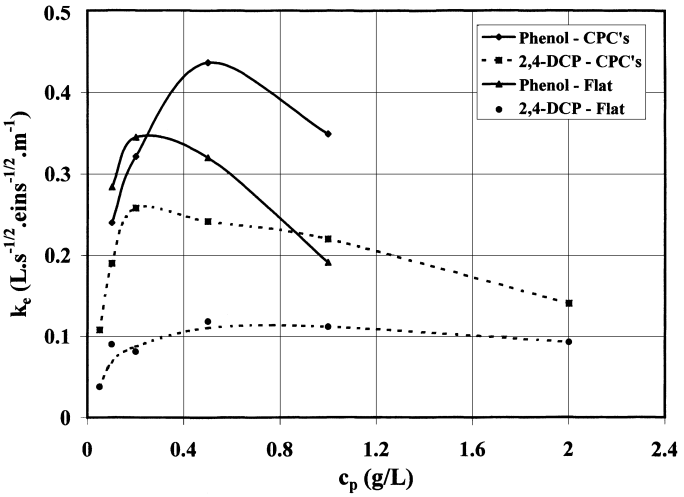

Fig. 9. Variation of kinetic constant (k_e) on catalyst concentration for experiments carried out in the flat reactor and in the CPCs modules with phenol and 2,4-DCP, and by considering that reaction rate is proportional to the square root of radiation entering (the same experiments than in Fig. 6).

flat) of the systems and the different radiation useful in each case.

Better comparisons can be made by calculating the quotients (ratios) between the kinetic constants obtained in the different reactors. Fig. 10 shows the results: each point is the quotient (ratio) of two kinetic constants obtained for two different experimental devices at the same catalyst concentration. Note that, if we use the kinetic constants (k) obtained by considering only time influence, it is not possible to establish a clear trend neither for phenol nor for 2,4-DCP. It can be seen that, in the phenol case, the quotient between the k obtained at CPCs and the k obtained at flat reactor increases when catalyst concentration does it, and it seems to go to a plateau. However, in the case of 2,4-DCP, the quotient between ks obtained at CPCs and flat reactor increases when catalyst concentration increases, but it reaches a maximum, and after that, decreases. Thus, it is not possible to establish a clear relationship between the two experimental devices tested, and it is difficult to determine what experimental device works better.

When the reaction rate is considered to be proportional to the square root of radiation entering, linear relationships have been obtained for the variation, with the catalyst concentration, of the quotients between k_e obtained at CPCs and k_e obtained at flat reactor. In the case of phenol treatment, the fitting of the variation of the quotients of the kinetic constants with the catalyst concentration drives to the following equations:

$$\frac{k_{e,CPC}}{k_{e,flat}} = 0.74 + 1.11c_p \quad (23)$$

It can be seen that the kinetic constants are also very close to each other. In any case, the influence of catalyst concentration has been minimized.

In the case of 2,4-DCP treatment, fitting of the variation of the quotients of the kinetic constants with the catalyst concentration allows us to obtain also a straight line, which equation is the following:

$$\frac{k_{e,CPC}}{k_{e,flat}} = 2.44 - 0.48c_p \quad (24)$$

As a conclusion, it can be said that the use of the kinetic constants calculated by considering the square root of the radiation entering minimizes the effect, on the reaction rate, of the radiation used, geometry of the photoreactor and catalyst concentration. An example can explain us the importance of this fact. If we observed Fig. 10, we can see that, in the case of 2,4-DCP treatment with a catalyst concentration of 0.5 g/l, the kinetic constant (k) obtained by considering only time is six times greater for CPCs than for flat reactor. However, if we compare the kinetic constants (k_e) obtained by considering that reaction rate depends on the square root of radiation, at the same catalyst concentration

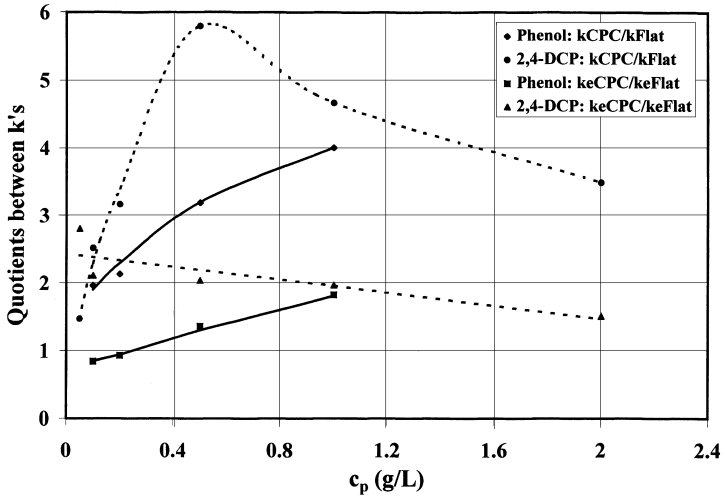

Fig. 10. Variation, on the catalyst concentration, of the quotient of the kinetic constants (k and k_e) for experiments carried out in the flat reactor and in the CPCs modules with phenol and 2,4-DCP, and by considering that reaction rate depends only on time or is proportional to the square root of radiation entering (quotients between data of Figs. 6 and 9).

$c_p = 0.5$ g/l, we can see that k_e for CPCs is only two times greater than k_e for flat reactor. Thus, if we use k in the design of photoreactor, it seems that volume of flat reactor has to be six times greater than volume of CPCs, and by considering the entering radiation (k_e) this proportion decreases to only two times. This means that we can make an error of 200% when we compare both reactors, and consequently, the introduction of radiation in the estimation of kinetic constant implies a considerable improvement in the design and in the minimization of errors in the scaling-up.

For the phenol case, a similar behaviour was observed. By considering also a catalyst concentration of 0.5 g/l, now, k obtained for CPCs is 3.2 times greater than this one obtained for flat reactor, whereas k_e is only 1.3 times greater for CPCs than for flat reactor.

The differences observed in the phenol and 2,4-DCP behaviour can be attributed to the different properties of these molecules which can influence, for instance, on their adsorption on the catalyst surface, their absorption of light, and evidently on the reaction rate.

Comparison between flat reactor and CPCs modules can be also made by calculating the collector area needed in each case to obtain the same conversion, that is the quotient S_{CPC}/S_{flat}.

We consider that reaction rate is proportional to the square root of the radiation entering the reactor because, then, closer values of kinetic constants for both systems (CPCs and flat reactor) have been obtained, as commented in the previous section. Equations (20) and (22) are useful to compare the evolution of concentrations. By setting a given conversion for both systems, the differences $\ln[c(t)] - \ln(c_0)$ have to be the same in the two equations. Thus, equalising Equations (20) and (22), it is obtained:

$$\frac{n_{\text{bmodC}}}{S_{\text{flat}}} = \frac{k_{\text{eF}}}{k_{\text{eC}}} \frac{K_{\text{F}}}{K_{\text{C}}} \frac{V_{\text{TC}}}{V_{\text{TF}}} \frac{W_{\text{TF}}^{1/2}}{W_{\text{TC}}^{1/2}} \tag{25}$$

Note that, in k_e, V_T and W_T, subindexes C and F have been added to indicate CPCs modules and flat reactor, respectively. K_C and K_F can be easily deduced from Eqs. (20) and (22) and they are, respectively:

$$K_{\text{F}} = \frac{1}{(N_{\text{a}} h c_{\text{v}})^{1/2}} \left(\sum_{\lambda=300}^{385} \lambda f_\lambda \right)^{1/2} \tag{26}$$

$$K_{\text{C}} = \frac{\Phi_{\text{ef}}^{1/2} S_{\text{bmod}}^{1/2} (n_{\text{Tmod}} \pi D L)^{1/2}}{(N_{\text{a}} h c_{\text{v}})^{1/2}} \left(\sum_{\lambda=300}^{385} \lambda f_\lambda \Phi_{\text{T}\lambda} \right)^{1/2} \tag{27}$$

The collector area needed for the CPCs modules (S_{CPC}) can be expressed as:

$$n_{\mathrm{bmodC}} = \frac{S_{\mathrm{CPC}}}{S_{\mathrm{bmodC}}} \tag{28}$$

and substituting in Eq. (25):

$$\frac{S_{\mathrm{CPC}}}{S_{\mathrm{flat}}} = \frac{k_{\mathrm{eF}}}{k_{\mathrm{eC}}} \frac{K_{\mathrm{F}}}{K_{\mathrm{C}}} \frac{V_{\mathrm{TC}}}{V_{\mathrm{TF}}} \frac{W_{\mathrm{TF}}^{1/2}}{W_{\mathrm{TC}}^{1/2}} S_{\mathrm{bmodC}} \tag{29}$$

k_{eC} and k_{eF} are related by Eq. (23):

$$k_{\mathrm{eC}} = k_{\mathrm{eF}}(0.74 + 1.11 c_{\mathrm{p}}) \tag{30}$$

This experimental equation can be introduced in Eq. (29):

$$\frac{S_{\mathrm{CPC}}}{S_{\mathrm{flat}}} = \frac{S_{\mathrm{bmodC}}}{0.74 + 1.11 c_{\mathrm{p}}} \frac{K_{\mathrm{F}}}{K_{\mathrm{C}}} \frac{V_{\mathrm{TC}}}{V_{\mathrm{TF}}} \frac{W_{\mathrm{TF}}^{1/2}}{W_{\mathrm{TC}}^{1/2}} \tag{31}$$

For comparison, it is assumed that the total volumes of both systems are equal. Thus, Eq. (31) becomes:

$$\frac{S_{\mathrm{CPC}}}{S_{\mathrm{flat}}} = \frac{S_{\mathrm{bmodC}}}{0.74 + 1.11 c_{\mathrm{p}}} \frac{K_{\mathrm{F}}}{K_{\mathrm{C}}} \frac{W_{\mathrm{TF}}^{1/2}}{W_{\mathrm{TC}}^{1/2}} \tag{32}$$

In the case of 2,4-DCP, the same explanations can be given, but in this case, k_{eC} and k_{eF} will be related by Eq. (24). Thus, Eq. (32) becomes:

$$\frac{S_{\mathrm{CPC}}}{S_{\mathrm{flat}}} = \frac{S_{\mathrm{bmodC}}}{2.44 - 0.48 c_{\mathrm{p}}} \frac{K_{\mathrm{F}}}{K_{\mathrm{C}}} \frac{W_{\mathrm{TF}}^{1/2}}{W_{\mathrm{TC}}^{1/2}} \tag{33}$$

The efficiency of every device depends on the daily weather. The incoming radiation to the systems is usually higher for the CPCs than for the flat reactor, being similar in cloudy days. In this sense, CPCs should be better. However, the fact that power number of both, W_{T}, is 1/2 attenuates the benefits of CPCs use.

For the same catalyst concentration, for instance 1 g/l, it results that, for a same degree of pollutant degradation, S_{CPC} area would be approximately one-third of that required for the flat reactor (assuming both W_{T} are equal). Nevertheless, this advantage does not lead to conclude that CPCs are better than flat reactor. We have also to consider the low energetic costs of the flat reactor (no pumping for suspension is required), almost null maintenance services (neither reflective surfaces nor tubes have to be cleaned) and simplicity of construction (less cost of immobilized capital).

All these factors seem to point out that flat reactors are a low cost alternative to the traditional concentrating systems. However, more extensive study on this system is necessary to establish the conditions in which it could be advantageously used in front of CPCs or other commercial systems.

4. Conclusions

Kinetics of photocatalytic degradation of phenol and 2,4-DCP, by using TiO_2 suspensions as catalyst, has been proved to be a first order reaction with respect to the phenol or 2,4-DCP concentration, in the range of catalyst concentrations tested (0–2 g/l).

Two kind of kinetic constants have been calculated. The first one by fitting evolution of phenol or 2,4-DCP concentration on time, and the second by fitting evolution of phenol or 2,4-DCP concentration on the square root of radiation entering. The values of these constants depend on catalyst concentration, utility used and kind of dependence of radiation. In the CPCs, kinetic constant increases when catalyst concentration does, reaches a maximum at 0.5 g/l, and after that decreases. In the flat reactor, kinetic constant also increases with catalyst concentration, and the maximum also appears here at 0.2 g/l.

Kinetic constants values for the two utilities tested have been compared. Important differences have been found when only dependence of phenol or 2,4-DCP concentration on time is considered. However, by considering the reaction rate depending on the square root of radiation entering, results improve. The closer constants values for the last case (reaction rate proportional to the square root of radiation entering) give an indication of the importance of including radiation entering in kinetic studies for photocatalytic processes. This inclusion means to take into account the geometry of the system (collector and reactor) and the catalyst concentration, minimizing and including their effects in the kinetic constant.

Finally, efficiencies of CPCs and flat reactor were compared attending to the collector area required to achieve the same phenol or 2,4-DCP conversion. From the experiments of this work, CPCs need a lower collector area than the flat reactor. At any rate, this conclusion could vary if weather changes (sunny or cloudy days), because the area criteria depend on radiation en-

tering the reactor. However, from the economical point of view, flat reactors are cheaper than CPCs and technically simpler (fabrication and maintenance). Thus, more accurate studies are needed in order to collect more data that help to clarify what system is better.

5. Nomenclature

c	reactants concentration
c_0	initial concentration
c_p	catalyst concentration
c_v	light rate
$c(t)$	concentration at time t
D	optical pathway
F_{abs}	radiation absorbed
F_e	radiation entering the system
F_i	radiation arriving at the system
f_λ	fraction of global radiation at wavelength λ
f(c)	function of reactants concentration
$f_a(F_{abs})$	function of radiation absorbed
$f_e(F_e)$	function of radiation entering the system
$f_i(F_i)$	function of radiation arriving at the system
h	Planck's constant
k	global kinetic constant
k_e	kinetic constant considering radiation entering the system
k_i	kinetic constant considering radiation arriving at the system
L	length of an illuminated tube
N_a	Avogadro's number
n_c	particles of catalyst illuminated
n_{mod}	number of modules of CPCs
n_{Tmod}	number of tubes in a CPCs module
r	intensive reaction rate
S_{col}	area of radiation collector
S_f	total area illuminated
S_{flat}	top area of flat reactor
S_{mod}	area of each CPCs module
t	time
V_T	total volume of the system
W_T	total radiation arriving at the system (from initial to final time)
$W_T(t)$	global radiation reaching the surface of collector at time t
X	conversion

6. Greek symbols

α_λ	absorption coefficient at wavelength λ
ϕ	quantum yield
Φ_{ef}	efficiency factor
$\Phi_{T\lambda}$	transmittance factors
λ	wavelength

Acknowledgements

Authors are grateful to the 'Comisión Interministerial de Ciencia y Tecnología (CICYT)' (projects AMB95-0885-C02-02 and AMB98-0357) and to the Spanish Ministry of Education ('Programa de Utilización de Grandes Instalaciones') (project UR1996-0042-01) for funds received to carry out this work. Authors are also grateful to Plataforma Solar de Almeria for the use of facilities, into the EC-DGXII TMR Program (Ref. ERBMFGE-CT-0023), and specially to Dr. Sixto Malato and Mr. Julián Blanco for their help and fruitful assistance during the experimental work at the PSA.

References

[1] D.F. Ollis, H. Al-Ekabi (Eds.), Photocatalytic purification and treatment of water and air, Elsevier Science Publishers, Amsterdam, 1993.
[2] O. Legrini, E. Oliveros, A.M. Braun, Chem. Rev. 93 (1993) 671.
[3] N. Serpone, E. Pelizzetti, Photocatalysis. Fundamentals and Applications, Wiley, New York, 1989.
[4] M. Schiavello (Ed.), Photocatalysis and Environment. Trends and Applications, NATO ASI Series, Series C. Mathematical and Physical Sciences, vol. 237, Kluwer Academic Publishers, Dordrecht, The Netherlands, 1988.
[5] H. Al-Ekabi (Ed.), The Third International Conference on TiO_2 Photocatalytic Purification and Treatment of Water and Air, Orlando, 1997.
[6] H. Al-Ekabi (Ed.), The 1998 European Workshop on Water and Air Treatment by Advanced Oxidation Technologies: Innovative and Commercial Applications, Lausanne, 1998.
[7] H. Al-Ekabi, N. Serpone, J. Phys. Chem. 92 (1988) 5726.
[8] V. Augugliaro, E. Davi, L. Palmisano, M. Schiavello, A. Sclafani, Appl. Catal. 65 (1990) 101.
[9] D. Bahnemann, D. Bockelmann, R. Goslich, Solar Energy Mater. 24 (1991) 564.
[10] Y. Mao, C. Schoeneich, K.D. Asmus, J. Phys. Chem. 95 (1993) 10080.
[11] R.W. Matthews, J. Phys. Chem. 91 (1987) 3328.
[12] R.W. Matthews, J. Catal. 113 (1988) 549.

[13] R.W. Matthews, Pure Appl. Chem. 64 (1992) 1285.
[14] A. Mills, S. Morris, J. Photochem. Photobiol. A: Chem. 71 (1993) 75.
[15] K. Okamoto, Y. Yamamoto, H. Tanaka, A. Itaya, Bull. Chem. Soc. Jpn. 58 (1985) 2015.
[16] K. Okamoto, Y. Yamamoto, H. Tanaka, A. Itaya, Bull. Chem. Soc. Jpn. 58 (1985) 2023.
[17] E. Pelizzetti, C. Minero, V. Carlin, New J. Chem. 17 (1993) 315.
[18] C.S. Turchi, D.F. Ollis, J. Catal. 122 (1990) 178.
[19] J. Blanco, S. Malato, Initial configuration of PSA solar detoxification loop, Report R 16-90, PSA, Almería, 1990.
[20] J. Blanco, Final configuration of PSA solar detoxification loop, Technical Report TR 06/91, PSA, Almería, 1991.
[21] J. Blanco, S. Malato, in D.E. Klett, R. Hogan, T. Tanaka (Eds.), Solar Engineering, The American Society of Mechanical Engineers, New York, 1994, p. 103.
[22] D. Curcó, S. Malato, J. Blanco, J. Giménez, P. Marco, Solar Energy 56 (1996) 387.
[23] D. Curcó, S. Malato, J. Blanco, J. Giménez, Solar Energy Mat. and Solar Cells 44 (1996) 199.
[24] J. Giménez, D. Curcó, P. Marco, Wat. Sci. Technol. 35 (1997) 207.
[25] C. Minero, E. Pelizzetti, S. Malato, J. Blanco, Chemosphere 26 (1993) 2103.
[26] M. Trillas, J. Peral, X. Domenech, J. Giménez, in: D.E. Klett, R. Hogan, T. Tanaka (Eds.), Solar Engineering, The American Society of Mechanical Engineers, New York, 1994, p. 171.
[27] C.V. Hsiao, C.L. Lee, D.F. Ollis, J. Catal. 82 (1983) 418.
[28] L. Borrell, S. Cervera-March, J. Giménez, R. Simarro, Solar Energy Mat. and Solar Cells 25 (1992) 25.
[29] S. Cervera-March, L. Borrell, J. Giménez, R. Simarro, J.M. Andújar, Int. J. Hydrogen Energy 17 (1992) 683.
[30] J. Sabaté, S. Cervera-March, R. Simarro, J. Giménez, Int. J. Hydrogen Energy 15 (1990) 115.
[31] J. Sabaté, S. Cervera-March, R. Simarro, J. Giménez, Chem. Eng. Sci. 45 (1990) 3089.
[32] S. Malato, J. Blanco, Ultraviolet radiation available for photochemistry at PSA, Technical Report R-3/93 SM/JB, PSA, Almería, 1993.
[33] D. Curcó, Kinetic and radiation models for photocatalytic processes, Doctoral Thesis, University of Barcelona, 1994.
[34] S. Cervera, J. Giménez, D. Curcó, M.A. Aguado, Study of the technical feasibility of the photocatalytical detoxification processes with concentrated solar light, Final Report to PSA, University of Barcelona, 1993.
[35] A.E. Cassano, Revista de la Facultad de Ingeniería Química, Santa Fe (Argentina) 37 (1968) 469.
[36] J.F. Rabek, Experimental Methods in Photochemistry and Photophysics, Part 2, Wiley, New York, 1982 (Chapter 27).
[37] M. Vicente, S. Esplugas, Afinidad 40 (1983) 453.
[38] C. Korman, D.W. Bahnemann, M.R. Hoffmann, Environ. Sci. Technol. 25 (1991) 494.
[39] M. Memming, Top. Curr. Chem. 143 (1988) 79.
[40] M.W. Peterson, J.A. Turner, A.J. Nozik, J. Phys. Chem. 95 (1991) 221.